Evidence for a Geomagnetic Wake at 500 Earth Radii

G. L. SISCOE,[1] F. L. SCARF,[2] D. S. INTRILIGATOR,[3] J. H. WOLFE,[4]
J. H. BINSACK,[5] H. S. BRIDGE,[5] AND V. M. VASYLIUNAS[5]

A comparison of the Explorer 35 solar wind plasma data with the data obtained by Pioneer 8 during a pass through the tail region at a geocentric distance of 500 R_E suggests the presence of a geomagnetic wake. The wake was characterized by a reduced density or increased temperature or both and by an almost unmodified flow speed as compared with upstream values. The change in density or temperature was of the order of 2 to 4. The wake is discussed in relation to the drag on the magnetosphere. A simple hydrodynamic calculation of wave drag effects gives approximate agreement with observed magnitudes, but the wake region appears to be somewhat larger than expected. Possible effects to account for this include heat diffusion out of the wake and a two-fluid effect in which ions are heated more than electrons at the bow shock. The data do not provide evidence for a viscous boundary layer in the usual sense, but a magnetic surface drag is not excluded. Finally, the possibility of local heating at the boundary is shown to be incapable of accounting for all wake features.

The extended geomagnetic tail is generally characterized by plasma, field, and wave properties that are distinct from interplanetary values. It is therefore possible to identify tail crossings from only local data collected from a single space probe. Some discrepancies in detail must be expected because the different experiments on one spacecraft use varying in-tail criteria or have disparate resolution characteristics. However, on Pioneer 8 the plasma probe observations [*Intriligator et al.*, 1969], the magnetometer measurements [*Mariani and Ness*, 1969], and the electric field characteristics [*Scarf et al.*, 1970] all suggested that the extended tail was intermittently encountered during the period of January 11 through January 28, 1968, with the greatest percentage of in-tail characteristics being given by the data of January 23.

A related question of fundamental interest concerns the possible existence of a geomagnetic wake region surrounding the extended tail. The appearance and behavior of the non-tail data obtained from Pioneer 8 during the period January 11 through January 28, 1968, are qualitatively similar to the characteristics of the interplanetary medium far from the earth, and the search for a wake cannot be made with only the local observations. Instead, we must compare in detail plasma measurements made upstream from the earth with non-tail data obtained in the vicinity of the extended tail. Here we report on the preliminary results of such a comparison made with solar wind data obtained upstream from the earth's bow shock from Explorer 35 and nearly simultaneous Pioneer 8 non-tail measurements.

The term 'geomagnetospheric wake' has sometimes been used to describe the entire disturbed region behind the earth [e.g., *Intriligator et al.*, 1969]. Our present definition of a tail crossing is described in detail at the beginning of the data comparison section. We restrict the term 'wake' to refer to the regions of disturbed solar wind flow that surround the tail crossings.

A comparison of upstream solar wind magnetic field with the near-tail field measured by Pioneer 7 at approximately 10^3 R_E downstream from earth has been presented by *Fairfield* [1968]. He found the field intensity near the tail to be smaller than the upstream value. A com-

[1] Department of Meteorology, University of California, Los Angeles 90024.
[2] Space Sciences Laboratory, TRW Systems Group, Redondo Beach, California 90278.
[3] Space Science Division, NASA Ames Research Center, Moffett Field, California 94035. Now at Department of Physics, California Institute of Technology, Pasadena 91109.
[4] Space Science Division, NASA Ames Research Center, Moffett Field, California 94035.
[5] Center for Space Research, Massachusetts Institute of Technology, Cambridge 02139.

plementary effect in the solar wind plasma is described and discussed in this report.

1. The Experiments

Pioneer 8 was launched into a solar orbit on December 13, 1967, on a trajectory that initially carried it beyond the earth's orbit. The projection onto the ecliptic plane of the near-earth part of the trajectory is shown in Figure 1. Between January 20 and January 25 the spacecraft passed through the expected position of the tail determined by extending a line from earth leeward at a nominal aberration angle. During this time the probe-ecliptic plane distance was less than 2 R_E. The interval under consideration extends from January 11 to January 30.

Solar wind plasma data on Pioneer 8 were obtained by a three-collector Ames Research Center (ARC) electrostatic plasma probe [*Intriligator et al.*, 1969]. The data have been subjected to a preliminary reduction that produces a three-parameter description of the plasma. A computer program to effect a more complete analysis of the data is currently being developed and tested.

The three parameters available for the present study are the peak velocity, the peak flux, and the flow direction in the equatorial plane of the spacecraft. For comparison with the Explorer 35 data, it is sufficient to use only the first two parameters. These parameters are obtained by first determining (by means of quadratic interpolation between measured values) the maximum current observed by the ARC probe and the corresponding value of energy per unit charge, and then dividing the current by the charge and probe area to obtain a flux and converting the energy per charge into a proton speed (see *Intriligator et al.* [1969] for details). The difference between the peak velocity so determined and the true solar wind speed depends on the plasma temperature, and it is typically of the order of 5% to 10%, with the peak velocity being the larger.

The ARC probe is designed to measure detailed energy spectra, and each energy channel normally covers only a small portion of the thermal energy spread of the solar wind ions. Consequently, the peak flux is normally a fraction (of the order of 0.1) of the total solar wind flux. For a given solar wind speed, the peak flux is proportional to plasma density and decreases with increasing temperature, since the temperature determines what fraction of the total solar wind flux the peak flux represents. Thus, at this stage in the data analysis, we do not explicitly separate density and temperature effects in any ordered program. However, the primary purpose here is to compare general upstream–downstream plasma characteristics, and for this the distinction is not crucial.

The Explorer 35 has monitored solar wind parameters continuously since it was injected into lunar orbit in late July 1967. This monitoring period includes the time of the tail passage of Pioneer 8. Of course, no solar wind data are obtained when the moon is in the geomagnetic tail, that is, around the times of full moon. Furthermore, even at the distance of the moon

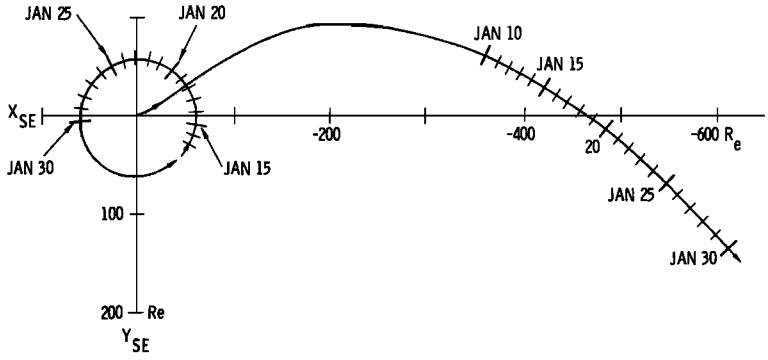

Fig. 1. Ecliptic projections of the trajectories for Explorer 35 in lunar orbit and the Pionner 8 interplanetary probe. The marks on the trajectory curves show the spacecraft locations at the start of each indicated day.

(approximately 60 R_E), the magnetosheath plasma is distinguishable from ambient solar wind plasma, but the difference is primarily in the plasma thermal speed. In any event, Explorer 35 plasma measurements are affected by the presence of the earth for approximately 4½ days on either side of the full moon. At other times, the data can generally be assumed to give true solar wind parameters. We are ignoring here the possibility of effects upstream of the earth's bow shock and the small fraction of the data affected by the lunar wake that have not been removed.

The Explorer 35 plasma data are obtained by a version of the Massachusetts Institute of Technology (MIT) Faraday cup. A description of the operational characteristics of this instrument, used on both Explorers 33 and 35, is given by *Lyon et al.* [1967]. The data have been subjected to a preliminary reduction program that produces the solar wind flow speed and direction, density, and thermal speed. The analysis is based on the assumption that the plasma can be adequately modeled by an isotropic Maxwellian distribution of particles. The reduction is preliminary in the sense that the α-particle density and proton temperature anisotropy have not yet been included. The thermal speed given by the present reduction does not account for a possible temperature anisotropy and is, therefore, intended as only a rough indication of the thermal condition of the plasma. The flow speed, density, and thermal speed are used in the present data comparison.

The position of Explorer 35 for January 12–30, 1968, is also shown in Figure 1. Since the two spacecraft were separated by approximately 500 R_E at the time of the tail encounter, we must be concerned about the time delay between changes in solar wind conditions that they observed. For solar wind structures moving outward with a nominal solar wind speed of 400 km/sec, we find a time delay close to 2 hours for the entire encounter interval. The structure would be observed first by Explorer 35. The data comparison will be made by using hourly averages, and a two-hour difference does not produce any difficulty.

2. Data Comparison

The five plasma parameters discussed in the previous section and other relevant information are displayed in Figures 2 and 3 for an 18-day interval that includes nearly all the tail encounters. In Figure 2 the upstream and downstream flow speeds are compared. Shown are the hourly range of Explorer 35 bulk flow speeds, the hourly range of the Pioneer 8 peak velocity, and the percentage of each hour Pioneer 8 was in the tail, as indicated by the on-board solar wind ion and VLF electric field detectors. Only Pioneer 8 data judged to be 'out of the tail' are included in the figure. If the following criteria were met the given spectrum was considered to be 'in the tail': (1) if the plasma energy spectrum resembled any of the basic disturbed spectra described by *Intriligator et al.* [1969, see especially Figure 4]; (2) if $j_{max} < 10^6$ ions/cm^2 sec; (3) if the angular distribution is highly erratic on a time scale compared with one plasma probe scan period (approximately 65 sec). We also display here hourly average and minimum values for the 400-Hz potential amplitudes. These electric field measurements clearly show where storms were encountered, and the very low minimum values are generally indicative of a tail crossing, as discussed by *Scarf et al.* [1970]. Pioneer 8 in-tail plasma probe data are not included in the central panels. The reader is referred to Figure 1 of *Scarf et al.* [1970] for a comparison of the Pioneer 8 magnetic field and broad-band electric field measurements for this interval and, also, for a discussion of the tail encounter data. Figure 4 of *Scarf et al.* [1970] also supplements the present Figure 2, since in that report peak values of the 400-Hz amplitudes are shown for January 18–30. Finally, the data on tail encounters from Figure 2 of that paper are also quite relevant to the present discussion.

Figure 3 gives the hourly range of the peak flux from Pioneer 8 and the related plasma parameters, hourly averages and standard deviations of the upstream density and thermal speed, from Explorer 35. The hourly percentage of tail encounters and the Pioneer 8 peak velocities are repeated here to help identify tail-associated features and storm phenomena.

Before comparing the two sets of plasma data, it is interesting to look in the Pioneer 8 data alone for signs of solar wind modification circumjacent to the tail, some of which were discussed by *Intriligator et al.* [1969]. Although tail encounters occurred throughout the interval,

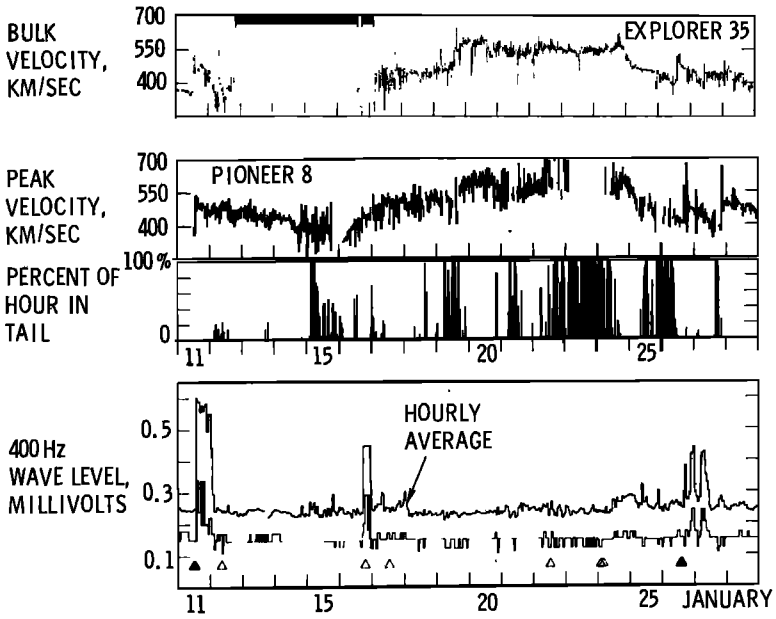

Fig. 2. Hourly samples of the upstream bulk velocity (Explorer 35) and downstream peak velocity (Pioneer 8) for January 11–28, 1968, with 400-Hz electric field data from Pioneer 8. The Pioneer 8 plasma probe observations are shown for only the periods when out-of-tail energy spectra were detected, and the per cent of each hour within the tail is displayed. The height of each line in the velocity panels represents the difference between the maximum and the minimum value measured during the hour. The solid and open triangles below the 400-Hz minimums show when sudden commencements and sudden impulses were detected on ground magnetograms, and several of these clearly correspond to the passage of interplanetary shocks. The dark horizontal bar on the Explorer 35 plot marks the period when the moon and spacecraft were within the tail region (see Figure 1).

the probability of encounter had a distinct maximum around January 23 and January 24. One reasonable interpretation is that this maximum represents the nominal location of the tail, which, however, suffers excursions to either side as a result of small variations in the solar wind direction. The empirical relation between the positions of the Pioneer 8 tail encounters and the solar wind direction is now under study. The asymmetry in the distribution might be related to the interplanetary disturbance that occurred on January 26.

Accepting this interpretation, we would expect any broad spatial feature associated with the tail to extend over several days and to be centered around the nominal tail position. Figures 2 and 3 show that both the peak flux and peak velocity have broad variations that maximize around January 23 and 24. For the peak flux there is a decrease, whereas the peak velocity shows an increase. Thus the variations in the data might suggest a broad circumjacent modification characterized by a decreased peak flux and increased peak velocity.

If this interpretation were true, it should also be reflected at each encounter that occurred away from the nominal position. That is, if encounters before and after the nominal tail position are due to motions of the tail over distances comparable to the apparent effect, the effect also should move with the tail. Thus there should be a decrease in peak flux and an increase in peak velocity before and after each encounter. These variations could be very brief if the speed of lateral motion of the tail is high. A close inspection of the figures reveals that there is, in fact, a tendency for the peak flux to be reduced adjacent to data gaps that represent tail encounters. However, the situation with regard to the peak velocity is not clear, and,

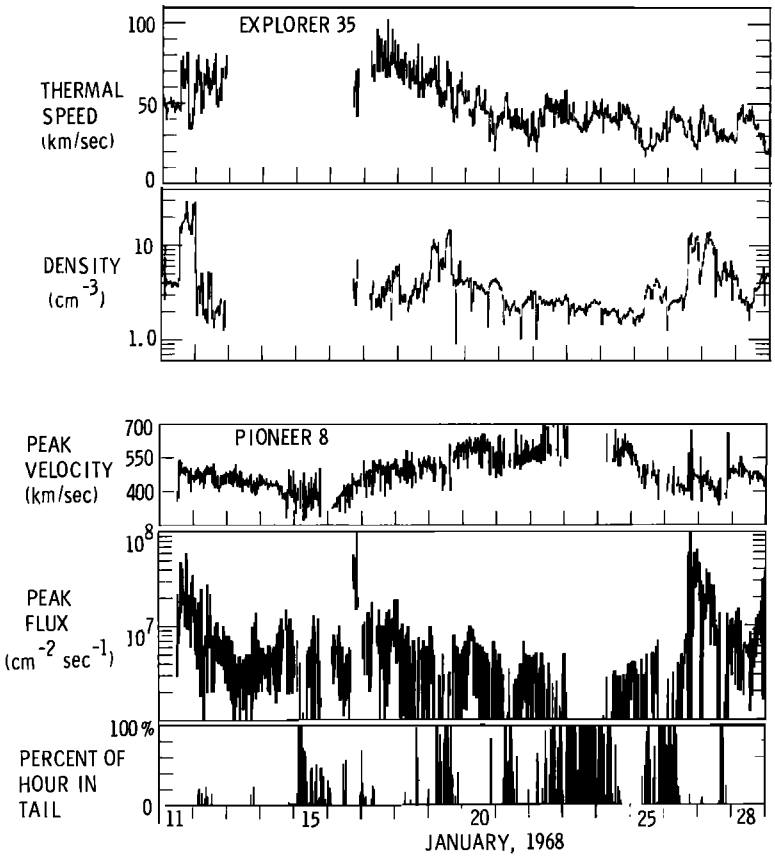

Fig. 3. Comparison of Explorer 35 plasma density and thermal speed with the range of peak flux from Pioneer 8. The Pioneer data are shown for out-of-tail points only. As a guide the Pioneer peak velocity and per cent of time in-tail panels from Figure 2 are repeated here. The Pioneer results represent hourly maximums and minimums. The upper curve in each Explorer 35 panel is the hourly average plus one-half the standard deviation, and the lower curve is the average minus half the standard deviation.

if there is a tendency for the velocity to be increased adjacent to data gaps, it is not very noticeable. Although the Pioneer 8 data suggest the presence of an effect, upstream solar wind data are needed to confirm the suggestion and to resolve the ambiguities.

Before we make this comparison, some preliminary comments on the Explorer 35 data are needed. The data gap between January 12 and January 17 is the result of the moon's passing through the geomagnetic tail. Full moon occurred on January 15; hence, the spacecraft was not upstream from the earth's bow shock until 4½ days later, or about January 19. The data from January 17, 18, and 19 are then mostly magnetosheath data, as evidenced particularly by larger values and variations in the thermal speed. The density drop and velocity rise on January 19 could be attributed to the crossing of the earth's bow shock, but we believe that this is not the cause for several reasons. It is too broad a feature for a shock crossing; the density drop precedes the velocity rise by at least one hour; a similar feature appears in the peak velocity of Pioneer 8; and, finally, on all other passes studied at this resolution the bow shock crossing could not be distinguished in the density or velocity data and could be distinguished only occasionally in the thermal speed data. The point of this discussion is that the upstream solar wind densities and velocities from January 19 onward are probably those

given by the Explorer 35 values, although the January 19 values included some magnetosheath data. The thermal speed should be used only from January 20 on.

A final comment on the Explorer 35 data concerns the occasional, but periodic, occurrences of anomalous values, generally being lower than neighboring values, in all three data fields. The interval between successive occurrences is approximately ½ day. These result from the inclusion of lunar wake data in the averaging. They are easily identified and should be excluded from the intended comparison.

We now compare the upstream and downstream data; we consider first the peak velocity and the bulk velocity (Figure 2). Here the correspondence between the details of the variations over the 10-day interval from January 19 to January 29 is quite good. The increase on January 19, the decrease the following day, the peak and subsequent drop on the January 24, the increase due to a shock wave on the January 26, and following structure occur in both data fields. In both data fields the general trend throughout the interval is nearly identical. The conclusion must be that the suspected tentative wake feature, detected from the peak velocity variation, is in fact a real variation in the solar wind speed.

The situation with the peak flux (Figure 3) is slightly more promising. We find in the interval between January 20 and 26 a broad depression with an amplitude of approximately a factor of 3 in the peak flux. However, the upstream density displays in the same interval a similar depression with an amplitude of approximately a factor of 2, and there is also a suggestion of an associated slight increase in the thermal speed. The upstream variations in density and thermal speed might therefore account for the broad peak flux depression. There are, however, also anomalously low peak fluxes directly adjacent to most of the tail encounter intervals, as mentioned earlier, and these are not obviously reflected in the upstream density and thermal speed variations. Thus this suggestion of an effect remains.

Without further analysis it is not clear that the peak fluxes measured around the tail are not those properly associated with the upstream plasma parameters. To see this we must compare data between the two spacecraft at times when no effects are expected, that is, after the tail encounters. To sharpen the comparison, we apply the following simple processing to the data. If we assume that the proton distribution function $f(\mathbf{v})$ can be adequately parameterized by the density N, bulk velocity $\mathbf{V}$, and thermal speed w (that is, $f(\mathbf{v}) = f[(\mathbf{v} - \mathbf{V})/w]$, ignoring thermal anisotropies), then, using the fact that for the electrostatic analyzer the response function depends only on angles and the ratio of the particle energy to the plate voltage, we obtain scaling laws for the peak quantities, namely

$$\text{Peak Flux} = NV\psi(w/V)$$

$$\text{Peak Velocity} = V\chi(w/V)$$

where ψ and χ are some functions of their arguments [*Vasyliunas*, 1970]. (For example, in the unrealistic case of an infinitesimally narrow response function, the peak flux is $\sim NV^4/w^3$ and the peak velocity is $\sim V + (4w^2/V)$, if the distribution is Maxwellian and $V \gg w$.) A useful method of comparison is then to plot the ratio peak flux at Pioneer 8 to NV at Explorer 35 against w/V for data near and away from the tail. If the plasma is unchanged between Explorer 35 and Pioneer 8, the points should all cluster near a curve, with the scatter away from that curve being a measure of statistical fluctuations and importance of neglected effects. If the data from the wake crossing period, plotted this way, are significantly different from the solar wind data, we can interpret the difference as evidence of a wake. We could also plot peak velocity/V against w/V as another check; however, the size of the expected effect is smaller than, or of the same size as, the hourly range of the peak velocity and, thus, the expected uncertainties are too large.

The results of this procedure are given in Figure 4. The open squares represent available data after the tail encounter interval, and these are presumably interplanetary. These data were obtained on January 28 and 29 and February 4. The storm that began on January 26 apparently carried the wake region eastward away from Pioneer 8, as no further tail encounters of significance were seen after January 27, and the data after this time do tend to cluster in a reasonably well defined manner in the figure.

The other points (solid dots) are from the January 20 to 26 interval. Earlier data were not used because of the magnetosheath crossing

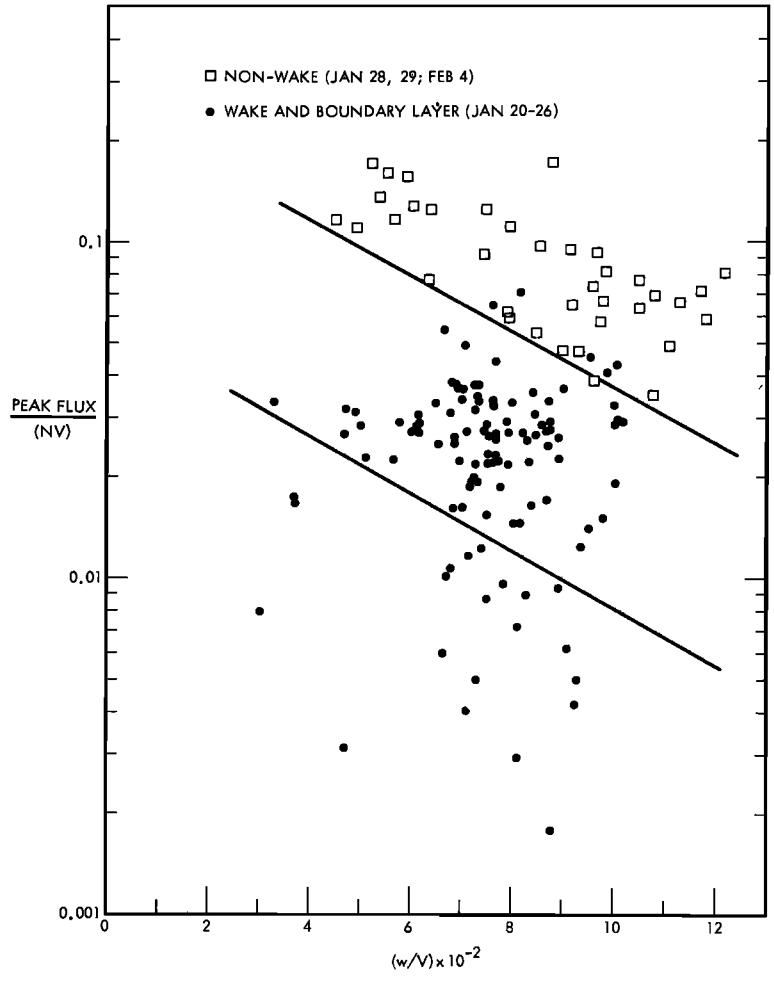

Fig. 4. Ratio of Pioneer 8 peak flux to Explorer 35 total flux NV as a function of the ratio of thermal speed w to bulk speed V. The data comparison involves Pioneer observations made two hours after those from Explorer, to account for the nominal time delay (see Figure 1). The lower than normal values for the flux ratio are interpreted in terms of wake effects, as described in the text.

of Explorer 35. We find that the suspected wake data do in fact cluster in a different region than the later data, and the difference suggests that for January 20–26 either the peak flux is lower than normal or the plasma temperature is elevated. We will argue later that both effects are probably acting.

An arbitrary division between the wake and non-wake data is suggested by the top solid line. The wake data include all the measurements in the January 20 to 26 interval except for a few points above the line, which all came at the end of the interval. Thus the wake region covers almost the entire interval. The lower solid line is another arbitrary division between the majority of the wake data and data with anomalously low peak fluxes. These are the anomalous values adjacent to most tail encounters pointed out earlier.

As a rough indication of the magnitude of the wake effect, we note that the data between the two solid lines differ from the non-wake data roughly by having one-quarter the density or twice the temperature, or some mixture of the two effects.

In summary, the comparison shows that dur-

ing the interval of from January 20 to January 26 the plasma data differ noticeably from the upstream or non-wake data, and that the difference is consistent with detection of a greater wake temperature, a smaller density, or both. In addition, there are intervals immediately adjacent to tail encounter with even larger reductions in peak flux.

The width of the wake at the distance of Pioneer 8 cannot be established with the present data because of interference of geomagnetic tail and magnetosheath with the Explorer 35 data on the one (early) side, and the occurrence of an interplanetary disturbance on the other (late) side. The problem of determining the actual profile of the wake is also complicated by the lateral motions of the tail, which are probably as large as the sensible wake. However, from Figure 1 we see that from January 20 to January 26 (the interval of reduced peak flux), Pioneer 8 moved a distance transverse to the earth-probe line of approximately 60 R_E, or 1.5 tail diameters (if the tail diameter at that distance was the same as near the earth, about 40 R_E), suggesting that the wake size is of the order of the tail diameter.

3. Discussion

The results of the previous sections bear directly on certain aspects of the solar wind–magnetosphere interaction. We compare here the observed solar wind behavior with that predicted from aerodynamic calculations of supersonic flows around elongated blunt bodies in which the bow shock determines the downstream behavior. We also consider a viscous boundary layer. Finally, we examine the possibility of local nonthermal heating at the tail boundary.

To place these topics in a proper context and to impose certain constraints on the present discussion, we briefly review relevant material from the general subject of magnetospheric dynamics. Downstream conditions are determined by the nature of the magnetospheric interaction, and they reflect exchanges of mass, momentum, and energy between the solar wind and magnetosphere. To a good approximation the mass exchange is negligible. The momentum exchange, which accounts for the drag on the magnetosphere, may be decomposed into wave drag and surface drag components. The wave drag is the usual force on the day-side magnetosphere due to the shock-compressed gas and, in fact, provides the power required to maintain the bow shock wave [*Landau and Lifschitz,* 1959]. The calculation of *Mead* [1964], based on a Newtonian interaction (known to provide a good approximation to the drag in hypersonic flow situations [*Hayes and Probstein,* 1959]), leads to a typical magnitude estimate of 2×10^7 newtons for nondisturbed conditions. To the extent that the wave drag does not actually move the magnetosphere, there is no energy exchange associated with this interaction.

A surface drag results from a tangential stress applied at the surface of the magnetosphere (the magnetopause). Favored agents to provide such a stress are viscosity [*Axford and Hines,* 1961; *Axford,* 1964] and magnetic forces [*Dungey,* 1961]. These authors relate the need for a tangential stress to high-latitude ionospheric phenomena. *Axford* [1964] has estimated the required magnitude to be approximately 2.5×10^6 newtons or about ⅛ of the wave drag. This estimate was subsequently confirmed by a more elaborate aerodynamic calculation [*Dryer and Heckman,* 1967] and by an independent method that gave directly the force between the earth and the geomagnetic tail [*Siscoe,* 1966]. A surface drag entails energy exchange, since the flow is slowed with consequent loss of kinetic energy. The above estimate of the surface drag magnitude implies an energy exchange rate of approximately 10^{12} watts. (For a discussion of consequences see the above references and *Siscoe and Cummings* [1969].)

The drag on the magnetosphere is applied directly on the earth by means of the magnetic field gradient established by boundary and tail currents in the vicinity of the earth [*Siscoe,* 1966]. This gradient has been measured for 30 geomagnetically quiet days in 1967 by use of magnetic data from the ATS 1 satellite in synchronous orbit (Cummings, Coleman, and Siscoe, unpublished data) [*Schieldge and Siscoe,* 1969]. Schieldge and Siscoe compare the gradient with simultaneous upstream solar wind plasma measurements to obtain the actual drag. The results show good agreement with the drag estimates given above and appear to exclude any other appreciable types of drag or appreciable upward revision of present drag estimates.

The above discussion imposes some constraints on the interpretation of the present results since the downstream measurements reflect the magnitudes of momentum and energy exchange rates. *Dryer and Heckman* [1967] have calculated the downstream flow parameters associated with the wave drag and with a viscous boundary layer. For the wave drag parameters they assumed a polytropic index γ of 1.2 and a Mach number of 3.8. These values are now regarded as being generally too low; however, the difference is not likely to affect the over-all flow structure, but rather will affect the specific magnitudes, which can be recalculated on the stagnation stream line to provide an indication of the revised magnitudes.

For the wave drag *Dryer and Heckman* [1967] show that the region of appreciable modification (greater than 10% when compared with upstream parameters) circumjacent to the tail extends approximately one tail diameter beyond the tail boundary. The greatest modification occurs at the tail boundary, which is the downstream continuation of the stagnation stream line. For the purpose of numerical comparison, we can estimate the difference in the upstream and downstream values of the solar wind parameters on the stagnation stream line attributable to the bow shock compression and subsequent expansion. To this end we use the equations of ordinary gas dynamic flows and shock waves, and, for simplicity, we ignore the solar wind magnetic field in the calculation.

Then by standard methods [*Liepmann and Roshko*, 1957], we find that the stagnation stream line parameters approach asymptotic values for large distances down the tail. Since 500 R_E is approximately 12.5 tail diameters, it is reasonable to assume that the asymptotic values are, in effect, attained at this distance. The parameters that enter the calculation are the bulk velocity V, the density ρ, and the temperature T. The ratios of the asymptotic values to the upstream values as a function of upstream Mach numbers are shown in Figure 5. We have used a polytropic relation between pressure and density of the form $p = \alpha\rho^\gamma$ and have taken the polytropic index $\gamma = 5/3$ for this calculation.

The figure shows that the bulk velocity is reduced from the upstream value by an amount of the order of 5% to 10%, and that the reduction is fairly insensitive to the Mach number. The density and temperature are inversely proportional to one another and are quite sensitive to the Mach number. A typical upstream Mach number is generally taken to be 8, for which the density is approximately one-fourth the upstream density and the temperature approximately four times the upstream temperature.

One recognizes similarities to the situation revealed by the Pioneer 8–Explorer 35 data. The velocity is nearly unchanged, as predicted. The downstream temperature is higher and the peak flux, which is proportional to the density, but inversely related to the temperature, is lower. In fact, near the tail boundary the density and temperature should be changed by one-fourth of the upstream value.

The region of reduced peak flux is roughly consistent with the calculation of Dryer and Heckman, but possibly is somewhat larger. This possibility is of considerable interest since it is generally difficult to increase the area of modified parameters appreciably without at the same time changing the net drag on the earth.

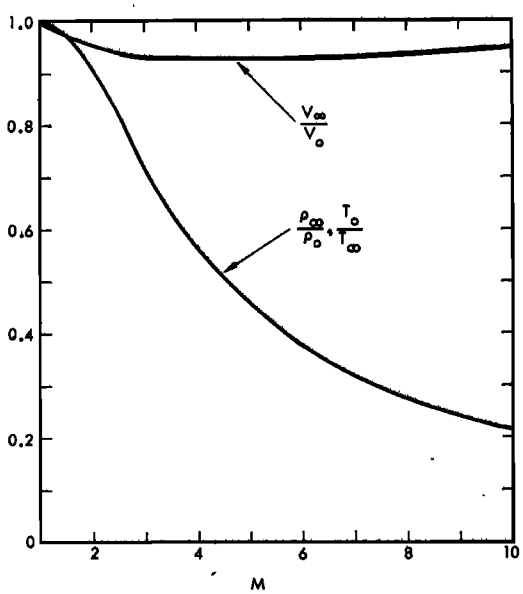

Fig. 5. Variation of parameters on the stagnation streamline as a function of Mach number M. The 0 subscripts refer to ambient solar wind velocity V, density ρ, and temperature T. Conditions far downstream from the shock are denoted by ∞ subscripts.

We therefore examine some specific possible mechanisms to increase the size of the affected region without requiring increased drag on the earth.

A simple possibility is suggested by the predicted temperature gradient. The temperature at the boundary is perhaps four times greater than the temperature one tail diameter away. Since heat can be conducted fairly readily along magnetic field lines, heat will flow away from the boundary extending the heated region, but the peak temperature will be reduced. The gas in the region heated by conduction will expand to maintain transverse pressure balance. Thus the peak flux is reduced by both the reduced density and increased temperature. However, the peak flux reduction near the boundary will then be less than that estimated without heat conduction.

A second possibility concerns the additional consideration required for a proper two-fluid treatment of the problem. In the one-fluid treatment of Dryer and Heckman the temperature is defined as proportional to the pressure-density ratio. In a two-fluid treatment the pressure is the sum of an electron and ion component. The data analysis given in the previous section concerns only the ion component, whereas the calculation concerns the sum of the two components. If there is any change of the pressure ratio between the two components as compared with the upstream ratio, the data and the calculation are not strictly comparable. Data from the Imp 1 satellite indicate that the ratio of the electron to proton pressure changes from greater than, to less than, one across the bow shock (the proton pressure is the greater on the shocked side) [*Olbert*, 1968]. Thus the velocity, density, and pressure profiles in the wake that determine the exchange rate of momentum and energy might be the same as calculated values, but the ion temperature might be higher (this being determined by details of the bow shock dissipation mechanisms) and the resulting peak flux lower, as observed.

However, this two-fluid effect is not free from the constraints mentioned earlier. *Von Kármán* [1954] originally pointed out that the wave drag is proportional to the rate of entropy generation in the entire shock wave. Thus, even though it is possible to increase the ion temperature at the expense of the electrons without changing the velocity, density, and pressure, the total entropy generated must also not change. The region of the proposed two-fluid effect is thereby constrained to be on streamlines that connect to the strong shock wave part of the bow shock where entropy changes are appreciable. We conclude that the effect can somewhat extend the region of reduced peak flux in two ways: one by simply extending the region of hot ions and the other by heating the ions at the boundary more than predicted and thereby giving more heat to be diffused into the surrounding medium.

It should be noted at this point that the present wake data could be simply accounted for by a combination of the above effects insofar as we have developed them. Since there is considerable uncertainty in the actual ion temperature and in the transverse dimensions of the observed features, the data are consistent with the general peak flux depression being attributable to the two-fluid effect and the anomalously low values to the wave drag modification since the latter can produce very low peak fluxes next to the boundary. However, as already mentioned, there are good reasons to suspect the presence of a boundary layer, and we should therefore also consider the surface drag component.

Just as a bow shock is the signature of wave drag, the surface drag signature is a boundary layer in which the exchanges of momentum and energy occur. By contrast, the wave drag effects are spread over the entire region between the body and the shock wave. Although the effects are greatest at the surface of the body, the greater area at large distances from the body more than compensates for the small size of the change in flow parameters.

Using the standard Prandtl boundary layer concept, *Dryer and Heckman* [1967] have calculated the characteristics of a magnetosphere viscous boundary layer. This calculation has a clear test in relation to the thickness of the boundary layer since, for a given drag, the thickness determines the average velocity in the layer, and this can be compared with Figure 2. Dryer and Heckman find at 500 R_E a boundary layer thickness of approximately 1.6 R_E. A lower limit on the average velocity defect in the layer (the difference between the actual veloc-

ity and the free stream velocity) can be found from a relation based on methods given in *Prandtl* [1952] for wake calculations (we have extended the integrals to the boundary instead of across the wake).

$$-\rho_0 V_0 \langle V_1 \rangle A_b \gtrsim D_b$$

where ρ_0 and V_0 are the free stream density and velocity, $\langle V_1 \rangle$ is the average velocity defect, A_b is the cross-sectional area of the boundary, and D_b is the total surface drag associated with the boundary layer. With $\rho_0 = 2.5$ cm^{-3}, $V_0 = 400$ km/sec, a boundary layer thickness of 1.6 R_E, a tail radius of 20 R_E, and $D_b = 2.5 \times 10^6$ newtons, we find $\langle V_1 \rangle \lesssim -200$ km/sec; that is, the average flow speed in the boundary layer is 200 km/sec less than the free stream speed.

There is no indication of sharply reduced values adjacent to the tail encounter in the hourly range for the peak velocity displayed in Figure 2. If such values did exist in a layer 1.6 R_E thick, they should have been observed as the plasma probe determined a peak velocity approximately every 60 sec. (If the lateral motion of the tail is due to nonradial solar wind flow components, the lateral speed should normally be less than 40 km/sec, corresponding to a 5° deviation of the flow from radial. Thus, a minimum of four measurements would be made in a 1.6-R_E layer.) It may be thought that a negative finding does not necessarily preclude a viscous boundary layer, since spectra with low V values could be mis-identified as part of the tail encounter data and be omitted from Figure 2. Several types of tail ion spectra were observed [*Intriligator, et al.*, 1969]. However, a review of the encounter data does not indicate the existence of a steady-state laminar viscous boundary layer in any obvious way. Further, since variations within a boundary layer are fairly continuous, the outer region should be transitional between free stream and encounter. Some data from this region could then be included in Figure 2, resulting in unusually low peak velocities near the boundary, but this is not observed. We conclude that the present data do not support the notion of a viscous boundary layer in the usual sense.

To retain the notion of a boundary layer supporting a drag of 2.5×10^6 newtons in the face of the present observations, the layer would have to be much thicker. We note that, if the surface drag is primarily due to a magnetic tangential stress, the stress would propagate into the flow at the appropriate hydromagnetic wave speed, rather than be confined to a narrow boundary layer. Consider a hydromagnetic wave speed of 50 km/sec and a streaming speed of 400 km/sec. Then at 500 R_E the momentum defect is distributed over a layer 60 R_E thick, and the average velocity defect is then 2 km/sec, which is almost unobservable. Thus, the data are consistent with a magnetic surface drag of the stated amount. Since the tail radius is of the order of 20 R_E, the large region affected by the magnetic stress might better be referred to as a boundary sheath than a boundary layer.

Another mechanism suggested by the VLF electric field measurements from Pioneer 8 could produce some of the wake features. The 400-Hz electric field data suggest there is dissipation occurring in the tail. A detailed study of these data [*Scarf et al.*, 1970] shows that dissipation is generally associated with discontinuities in the plasma or magnetic field, such as at the tail boundary or at null sheets. The dissipation heats the plasma, and, if the heat diffuses into the plasma surrounding the tail, the gas would expand laterally away from the tail and, thus, would reduce the density. This effect could then tend to account for the anomalously reduced peak fluxes. However, a rough estimate of the amount of heat required suggests that it cannot account for the broad region of reduced peak flux. (The effects due to the motion of the tail make this assessment somewhat uncertain.) The energy stored in the volume of reduced peak flux can be estimated by considering the work done to expand a gas from ambient solar wind conditions to this volume with its reduced density at constant pressure. If A_W is the area of the region with appreciably reduced peak flux, a simple calculation gives $PA_W(N - N')/N$ as the stored energy per unit length along the tail, where N is the ambient density, N' is the reduced density, and p is the pressure. The data suggest that a reasonable value for $(N - N')/N$ might be $\frac{1}{2}$, and that the stored energy per unit length is of the order of $\frac{1}{2}pA_W$. The magnetic energy per unit length stored in the tail is pA_T, where A_T is the area of the tail if we assume that the solar wind pressure outside the tail is balanced by the magnetic pressure inside. Thus,

to account for the observations by this mechanism, more energy would have to be dissipated than is stored in the tail at 500 R_E. The magnetic field intensity within the tail was measured to be approximately 6 γ [*Mariani and Ness*, 1969], which is not much different than the typical tail field at the distance of the moon ($\sim$8 γ) [*Mihalov and Sonett*, 1968].

Hence, the energy density at 500 R_E is comparable to that at 60 R_E. Also, Figures 1, 2, and 3 suggest that the volumes involved at 500 R_E are as large as, or larger than, the tail volume at 60 R_E. Thus there appears to be insufficient energy within the tail at 60 R_E to provide for the tail and wake energies at 500 R_E. We conclude that the major features of the observed wake are probably the result of drag effects rather than local conversion of tail energy into heat by dissipation mechanisms.

Acknowledgments. We wish to thank M. Dryer and D. D. McKibbin for helpful discussions and A. Cowen for assistance in processing the large amount of data.

The research described here was primarily supported by the national Aeronautics and Space Administration under NAS 2-4673 (TRW), and NGR-22-009-372, and NGL-22-009-015 (MIT).

* * *

The Editor wishes to thank D. H. Fairfield and J. R. Spreiter for their assistance in evaluating this paper.

References

Axford, W. I., Viscous interaction between the solar wind and the earth's magnetosphere, *Planet. Space Sci., 12*, 45, 1964.

Axford, W. I., and C. O. Hines, A unifying theory of high latitude geophysical phenomena and geomagnetic storms, *Can. J. Phys., 69*, 1181, 1961.

Dryer, M., and G. R. Heckman, On the hypersonic analogue as applied to planetary interaction with solar plasma, *Planet. Space Sci., 15*, 515, 1967.

Dungey, J. W., Interplanetary magnetic fields and the auroral zones, *Phys. Rev. Lett., 6*, 47, 1961.

Fairfield, D. H., Simultaneous measurements on three satellites and the observation of the geomagnetic tail at 1000 R_E, *J. Geophys. Res., 73* (17), 6179, 1968.

Hayes, W. D., and R. F. Probstein, *Hypersonic Flow Theory*, Academic, New York, 1959.

Intriligator, D. S., J. H. Wolfe, D. D. McKibbin, and H. R. Collard, Preliminary comparison of solar wind plasma observations in the geomagnetospheric wake at 1000 and 500 earth radii, *Planet. Space Sci., 17*, 321, 1969.

Landau, L. D., and E. M. Lifschitz, *Fluid Mechanics*, Addison-Wesley, Reading, Mass., 1959.

Liepmann, H. W., and A. Roshko, *Elements of Gas Dynamics*, John Wiley, New York, 1957.

Lyon, E. F., H. S. Bridge, and J. H. Binsack, Explorer 35 plasma measurements in the vicinity of the moon, *J. Geophys. Res., 72*(23), 6113, 1967.

Mariani, F., and N. F. Ness, Observations of the geomagnetic tail at 500 earth radii by Pioneer 8, *J. Geophys. Res., 74*(24), 5633, 1969.

Mead, G. D., Deformation of the geomagnetic field by the solar wind, *J. Geophys. Res., 69*(7), 1181, 1964.

Mihalov, J. D., and C. P. Sonett, The cislunar geomagnetic tail gradient in 1967, *J. Geophys. Res., 73*(21), 6837, 1968.

Olbert, S., Summary of experimental results from the MIT Detector on IMP-1, in *Physics of the Magnetosphere*, edited by R. L. Carovillano, J. F. McClay, and H. R. Radiski, p. 641, D. Reidel, Dordrecht, Holland, 1968.

Prandtl, L., *Essentials of Fluid Dynamics*, Hafner, New York, 1952.

Scarf, F. L., I. M. Green, G. L. Siscoe, D. S. Intriligator, D. D. McKibbin, and J. H. Wolfe, Pioneer 8 electric field measurements in the distant geomagnetic tail, *J. Geophys. Res., 75*(15), 3167, 1970.

Schieldge, J. P., and G. L. Siscoe, Aerodynamic factors of the magnetosphere (abstract), *Trans. AGU, 50*, 662, 1969.

Siscoe, G. L., A unified treatment of magnetospheric dynamics with applications to magnetic storms, *Planet. Space Sci., 14*, 947, 1966.

Siscoe, G. L., and W. D. Cummings, On the cause of geomagnetic bays, *Planet. Space Sci., 17*, 1795, 1969.

Vasyliunas, V. M., Deep Space Plasma Measurements, in *Methods of Experimental Physics*, edited by H. R. Griem and R. H. Lovberg, Academic, New York, 1970.

Von Kármán, T., *High Speed Aerodynamics and Jet Propulsion*, vol. 6, edited by W. R. Sears, Princeton University Press, Princeton, N. J., 1954.

(Received March 9, 1970;
revised May 5, 1970.)